Article

Noninvasive Colorimetric Detection of Acetic Acid in Human Breath Based on an Alginate/Ni−Al-LDH/Dye Composite Film

S. Amirabbas Zakaria, M. Hassan Amini,* and S. Hamid Ahmadi*
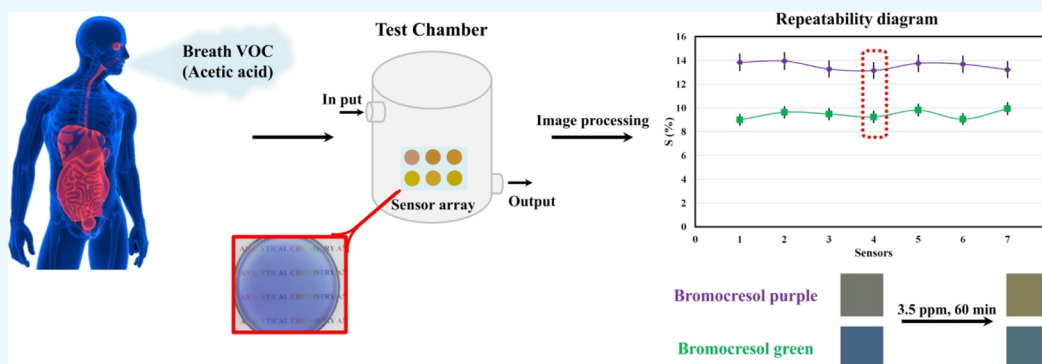
Read Online

ACCESS | Metrics & More | Article Recommendations | Supporting Information

ABSTRACT: Alginate/Ni−Al-layered double hydroxide/dye (Alg/Ni−Al-LDH/dye) composite films were fabricated using the solution casting method. The dyes used included methyl red, phenol red, thymol blue, bromothymol blue, *m*-cresol purple, methyl orange, bromocresol purple (BP), and bromocresol green (BG) in the overall pH range of 3.8 to 9.6. The chemical composition and morphology of the Alg/Ni−Al-LDH/dye composite film structure were investigated by Fourier transform infrared spectroscopy, FESEM, atomic force microscopy, and X-ray diffraction. The Alg/Ni−Al-LDH/dye composite films were semitransparent and mechanically flexible. Acetic acid was investigated as a respiratory biomarker related to gastrointestinal diseases. The parameters studied included color volume, response time, Ni−Al-LDH nanosheet volume, reusability, and drawing of the calibration curve along with statistical features including standard deviation, relative standard deviation, limit of detection, and limit of quantitation. Colorimetric indicators BP and BG in the presence of acetic acid produce color changes that are almost visible to the naked eye. However, other used indicators have shown almost no change. Therefore, it can be reported that the sensors made in the presence of BP and BG act selectively in relation to acetic acid.

1. INTRODUCTION

Noninvasive disease diagnosis is a rapidly developing strategy based on the analysis of volatile organic compounds (VOCs) emitted from various body sources (such as breath, skin, urine, and blood).[1−3] In 1971, Pauling et al.[4] identified more than 250 different VOCs in human breath. Therefore, human breath is a complex volatile mixture. However, the main VOCs of human breath in healthy individuals include methanol (160−2000 ppb), ethanol (13−1000 ppb), acetone (1.2−900 ppb), isoprene (12−580 ppb), and ammonia.[5] Jalal et al.[6] have reported that internal conditions, environmental exposure, diet, and lifestyle of individuals affect the concentration ratio of VOCs of a person, so the concentration ratio of VOCs can be different from person to person. A higher than average VOC concentration, without considering individual characteristics, indicates disease in the body. Therefore, the increase in VOC concentration is considered as a breath biomarker in disease diagnosis.[7]

Various techniques and methods are used to detect and measure the VOCs, including chromatography and mass spectrometry-based methods [such as gas chromatography (GC), GC−mass spectrometry, and proton transfer reaction− mass spectrometry (PTR-MS)].[8−10] Laboratory methods have appropriate sensitivity and reproducibility. However, from the point of view of the application, they require a professional operator and operating space and are undesirable for real-time and field use.[9] Colorimetric methods have attracted the attention of researchers as an alternative approach.[11] The main problem of colorimetric methods is the environmental influence on the quality of the results.[12] For example, breath colorimetric sensors may report an incorrect response when affected by humidity. Therefore, it is necessary to create a

structure with the least influence and higher selectivity for important breath markers.

It is well known that ambient humidity has little effect on gas sensors based on layered double hydroxide (LDH) structures.[13,14] This phenomenon can be related to the presence of interlayer water molecules in the LDH structure.[15] Therefore, an efficient sensor can be provided by using this inherent property in the measurement of breath markers. On the other hand, LDH nanosheets, as a protective layer, keep the pH indicators safe from environmental changes,[16,17] thus increasing the lifetime of the sensor. It should be noted that in addition to the protective role, LDH nanosheets can act as a barrier to prevent the rapid and timely penetration of the analyte into the inner layers.[18−20] Therefore, it is of particular importance to create a structure with proper permeability, stability, repeatability, and reproducibility.

In this study, alginate polysaccharide was used as a substrate with an egg-box structure and LDH as a polymer filler along with pH indicators by the solvent casting method. The performance of the sensor was evaluated by the colorimetric technique.

LDH nanosheets have been used as a key component of the composite structure to control the H- or J-arrangement of dye molecules.[16,17] Alginate has created a clear substrate and traps dye molecules within its chain−chain junction zones. Therefore, it can be ensured that the dye molecules have spread almost uniformly on the entire surface. In the next step, acetic acid as an important breath biomarker was investigated to evaluate the possibility of using a sensor array based on the Alg/Ni−Al-LDH/dye composite film in medical breath analyzers. The functional characteristics of sensors investigated by digital colorimetric and image processing techniques can be mentioned as sensitivity, response time, relative humidity (% RH) effect, repeatability, and reproducibility. Other investigated parameters include the limit of detection (LOD), limit of quantitation (LOQ), standard deviation (s), and relative standard deviation (RSD).

2. RESULTS AND DISCUSSION

It is well known that LDH nanosheets can act as a protective layer against light radiation. In this regard, Zhang et al.[17] mentioned that the structure of LDH nanosheets acts as a protection against the photoisomerization of azobenzene against light radiation. In general, dye molecules or ions on an adsorbent substrate can adopt two spatial structures. Wang et al.'s[16] arrangement of aggregates can be considered as H- (parallel arrangement and face-to-face arrangement) and J- (axial head-to-tail arrangement) form states. They have also reported that the interaction between dye molecules is relatively fragile and changes under the influence of the surrounding environment. Therefore, they have proposed the use of the LDH structure by the LB method as a self-assembly unit to produce an LDH/dye composite structure in a stable and regular manner. In this structure, natural red and rhodamine B were used to investigate hydrochloric acid and ammonia. In this way, by using the characteristic of binding and interaction of dye molecules with each other, in this present research, we have manufactured an Alg/Ni−Al-LDH/dye composite film structure with the approach of identifying breath volatile cancer markers. A composite film based on biological biopolymers (such as polysaccharides) provides flexibility and high efficiency. Therefore, it is necessary to consider the characteristics of the final composite film structure. The dye used was bromocresol purple (BP), which has a yellow-to-purple color change at a pH of 5.2−6.8. Therefore, it is necessary to design the structure of the composite film in such a way that the final film is placed in the basic range (purple range, pH higher than 6.8). Next, the quality of the produced composite film structure was examined.

2.1. Characterization of the Composites. Alginate polysaccharide-based films are used with glycerol as a plasticizer and calcium ions as the cross-linker.[21] It should be noted that LDH nanosheets can be used as polymer fillers and at the same time cross-linkers, and they further strengthen the final structure.[22,23] So, the effects of the proximity of these components together on the quality of the film were investigated. Ca^{2+} ions were used in amounts of 0 to 5 wt % by weight of alginate. According to the results, with the increase in the amount of added Ca^{2+} ions, the film turns yellow and becomes denser (Figure S3a, 1 to 5 wt %). Also, Ca^{2+} ions in amounts higher than 2 wt % lead to the turbidity of the film. The Ca^{2+} ion-free film (Figure S3a, 0 wt %) is purple, and it has lower strength, higher flexibility, and transparency than Ca^{2+} ion-containing samples. Therefore, Ca^{2+} ions were removed in the continuation of the work.

As mentioned earlier, BP dye was used in the manufacturing of the composite. In this structure, dye molecules can be considered as surface active sites for pollutant adsorption and recognition agent. Therefore, the optimal amount of dye that can be used in making the composites was investigated. Figure S3b shows the films obtained as a result of adding the dye solution in quantities of 0 up to 2 mL. According to observations, the darkness of the film increased with the increase in the volume of the dye solution, which indicates the increase of surface active sites and probably the higher ability to change color in the presence of pollutants. As can be seen in Figure S3b, the color in the volume of 2 mL was more chromatic than the other samples, but this volume of color in the film led to a decrease in strength and the film became unusable to some extent. On the other hand, the amounts of 0.5 and 1.5 mL of color have led to an increase in the turbidity of the final film. Therefore, color was used in the volume of 1 mL.

It is possible to say that the amount of added LDH is a key component for the formation and achievement of the highest performance of the composite. The structure of LDH leads to the orientation of dye molecules and creates a desired structure. Thus, LDH was examined in amounts of 4 to 9 mL. The results are shown in Figure S3c. The color of the composite films was not suitable for amounts lower than 6 mL of the LDH suspension. Also, the obtained films were turbid in amounts higher than 6 mL of the LDH suspension, while in the amount of 9 mL, the film changed color. Therefore, the volume of 6 mL of the LDH suspension was used in the continuation of the work.

Figure S3d shows the fundamental mechanical properties of the composite films. The pure Alg film has the lowest Ts (tensile strength). The addition of Ca^{2+} ions increased Ts and decreased elongation at break (EAB) compared to pure Alg. With the addition of Ni−Al-LDH, the tensile strength decreased to 118 ± 5 MPa, while the EAB increased to 32%. It can be considered that although the LDH structure does not increase the strength to the level of Ca^{2+} ions, it leads to the creation of a film with greater tensile strength. Also, the addition of dye [BP and bromocresol green (BG)] causes a decrease in Ts by about 10 MPa, which can be related to the creation of covalent bonds of the LDH structure with the dye molecules.[24]

The characteristic of the LDH colloidal suspension was investigated by the Tyndall effect.[25] In this method, the laser beam is irradiated transversely into the solution (section "LDH Nanosheets Preparation"), and when the laser beam passes

through the LDH colloidal suspension, a recognizable path is observed as a result of light scattering (Figure 1). According to
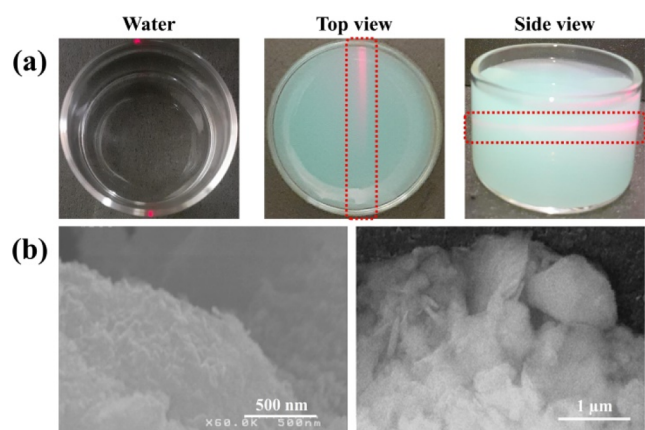

Figure 1. (a) Tyndall effect of the Ni−Al-LDH colloidal suspension (section "LDH Nanosheet Preparation") and (b) FESEM images of Ni−Al-LDH powder.

the obtained results, the LDH colloidal suspension has good stability, which is consistent with the results obtained by Rahman et al.[26] Also, the FESEM images of the LDH colloidal suspension are given in Figure 1b. According to the figure, it is possible to see LDH nanosheets separated from each other, which have a thickness of less than 100 nm.

FESEM images were used to investigate the microstructure and morphology of the composite film (Figure S4). According to Figure S4a, the structure of the pure Alg film has a thickness of about 27 nm with a distinct grain boundary (Figure S4a(II)). In the next step, with the addition of Ca^{2+} ions, despite the increase

in the thickness of the film, its texture becomes more dense, which can be related to the formation of the egg-box structure. Also, the formation of a compact and dense structure is a characteristic of calcium alginate films, which indicates the involvement of Ca^{2+} ions in the alginate polymer chain.[27] By adding Ni−Al-LDH, the composite film becomes denser and it has a smoother surface than the previous samples. However, according to the visual results that were mentioned earlier, the presence of Ca^{2+} ions was a destructive factor in the preparation of the final composite. In the next step, the Alg/Ni−Al-LDH composite is investigated (Figure S4d). LDH-shaped crystalline nanosheets can be seen in Figure S4d(II). In the final step of the composite manufacturing, by adding BP and BG dyes (Figure S4e,f, respectively), the films are obtained with a more uniform structure than the previous samples. As can be seen, the Alg/Ni−Al-LDH/BP composite has a thickness of 40 nm and the thickness of the Alg/Ni−Al-LDH/BG composite film is similar to that of the pure Alg film (Figure S4a(I)), and it maintains its dense and uniform texture.

Atomic force microscopy (AFM) analysis ($30 \times 30 \ \mu$m) was performed to obtain quantitative and qualitative (morphology) information, including the average roughness (R_a: average of the absolute value of the height deviations from a mean surface) and root-mean-square roughness (R_q: root-mean-square average of height deviations taken from the mean data plane) as quantitative and qualitative parameters, respectively. The calculated values of the quantitative parameters are shown in Figure S4. As shown in Figure S4, differences in morphology and average roughness can be observed, which can be attributed to the formation of a biopolymer network within the film in the presence of different dyes. Since R_a and R_q follow a consistent trend in the fabrication of composite films, R_q was investigated. According to the results, the pure Alg film has a R_q equal to 192
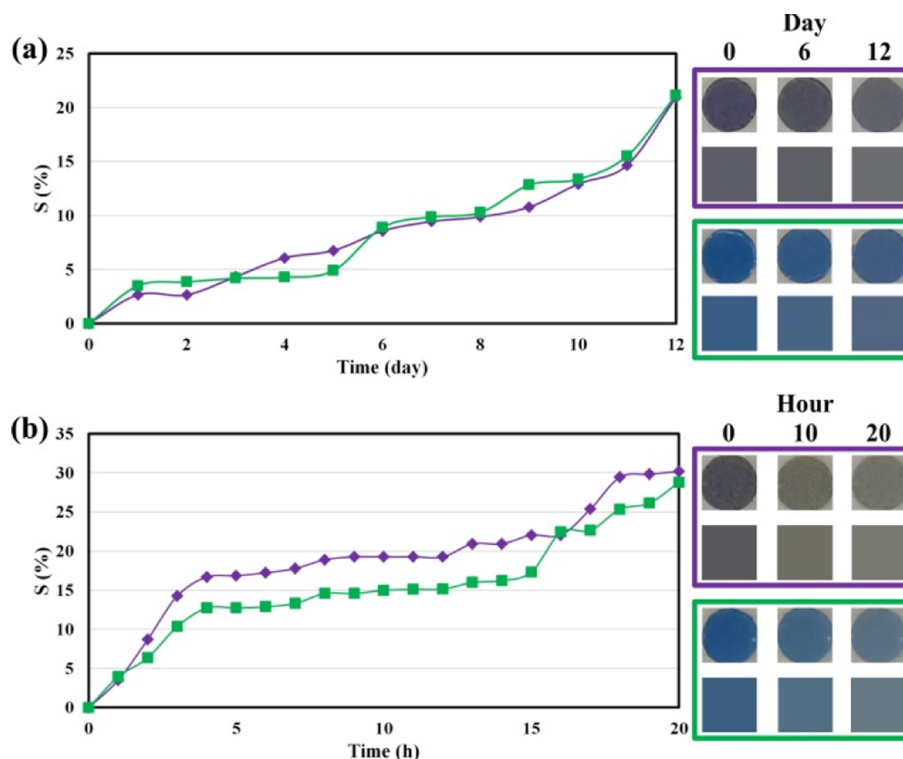

Figure 2. Color changes of the Alg/Ni−Al-LDH/dye composite films under (a) visible and (b) UV light (purple ◆ BP, green ■ BG) {the sensor response [S_{RGB} (%) = S (%)]}.
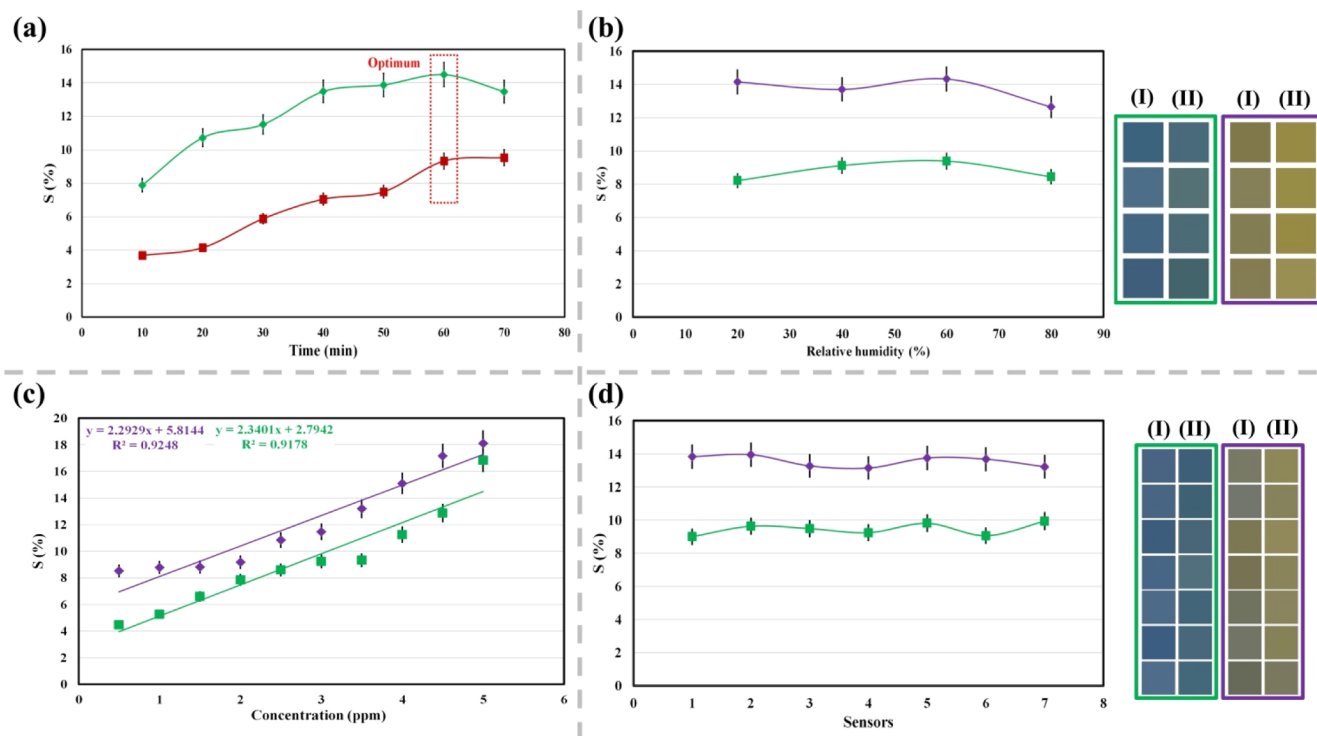
Figure 3. (a) Time optimization diagram [at con. 3.5 ppm, time 10−70 min and ambient temperature (green ◆ BP and red ■ BG)], (b) relative humidity diagram (inset: image) [at con. 3.5 ppm, time 60 min, and ambient temperature (purple ◆ BP and green ■ BG)], (c) calibration curve {at con. 0.5−5 ppm, time 60 min, and ambient temperature [(purple ◆) Alg/Ni−Al-LDH/BP and (green ■) Alg/Ni−Al-LDH/BG]}, and (d) repeatability diagram (inset: image) colorimetric sensor-based Alg/Ni−Al-LDH/dye composite films [at con. 3.5 ppm, time 60 min, and ambient temperature (purple ◆ BP and green ■ BG)] {the sensor response [S_{RGB} (%) = S (%)]}.

nm. With the addition of Ca^{2+} ions and LDH nanosheets, the R_q increased to 296 and 267 nm, respectively (both compared to the pure Alg film). It can be considered that the presence of Ca^{2+} ions and LDH nanosheets separately or together in the Alg film significantly increases R_q (according to FESEM results, the thickness of the film also increases in both cases). However, after the addition of dye, the R_q compared to that of the pure Alg film decreases by about 50%, which is also consistent with the FESEM results.

Figure S5 shows the X-ray diffraction (XRD) pattern of the compounds. The pure sodium alginate presented two weak and broad peaks around 14 and 23°, indicating a rather amorphous structure.[28] All diffraction peaks in Figure S5b can be attributed to the Ni−Al−NO$_3$ LDH hydrotalcite phase.[29] The sharp peaks situated at around 2θ = 11.08, 22.79, 34.61, 39.53, 46.37, 60.59, and 61.52° may correspond to the (003), (006), (012), (015), (018), (110), and (113) planes of Ni−Al LDH, respectively. By comparing the XRD pattern of the LDH structure and composites, it can be seen that the peaks corresponding to the (012), (018), and (113) planes have shifted to the left. Possible reasons include the creation of covalent and van der Waals bonds between the alginate and LDH nanosheet structure.

The Fourier transform infrared (FTIR) spectrum was used to investigate surface hydrogen bonding and electrostatic interaction between composite components in the range of 400−4000 cm^{-1} (Figure S5). The spectra of Ni−Al−NO$_3$ LDH powder and the alginate film are shown in Figure S5e. The broad absorption band in the range of 3100 to 3600 cm^{-1} indicates the stretching vibration of O−H (in the LDH structure, it can be assigned to the stretching mode of hydroxyl groups of brucite-like layers and interlayer water molecules). The sharp band in

1383 cm^{-1} and the small absorption band in 1637 cm^{-1} in the Ni−Al−NO$_3$ LDH spectrum are attributed to the stretching vibration of interlayer nitrate ions and the bending vibration of water molecules, respectively.[29] By comparing the pure LDH spectrum and the Alg/Ni−Al−NO$_3$ LDH composite film (Figure S5f), it can be stated that the stretching vibration of the O−H has been somewhat suppressed and shifted due to the formation of the hydrogen bond network between the LDH and Alg.[30−32] Also, the high intensity indicates a large number of hydroxyl groups and interlayer water molecules in the structure of the composite film. The bands at 2925, 1624, 1424, and 1039 cm^{-1} are assigned to asymmetric stretching vibrations, asymmetric and symmetric stretching vibrations of the carboxylate group, and C−O−C stretching groups, respectively.[33,34]

In this study, the effect of visible and UV light on the quality of the composite film was tested. Figure 2 shows the color changes in the films during a period of 12 days (Figure 2a) and 20 h (Figure 2b) under visible and UV light, respectively. According to the results, the composite film has good color stability against UV light for up to 5 h, and after that, the intensity of color degradation increases. Under visible light, the composite has good color stability for up to 15 days. Color stability in both cases can be related to the effect of the presence of LDH nanosheets in the composite film structure. In general, LDH has a good performance as a barrier to UV and visible light and it reduces the intensity of vulnerability to UV−visible light.[35]

According to the obtained results, the pure alginate film does not have good transparency (about 4%). The addition of Ca^{2+} ions increases the transparency of the film at 400 nm to about 14%. However, as explained earlier, it was not used due to
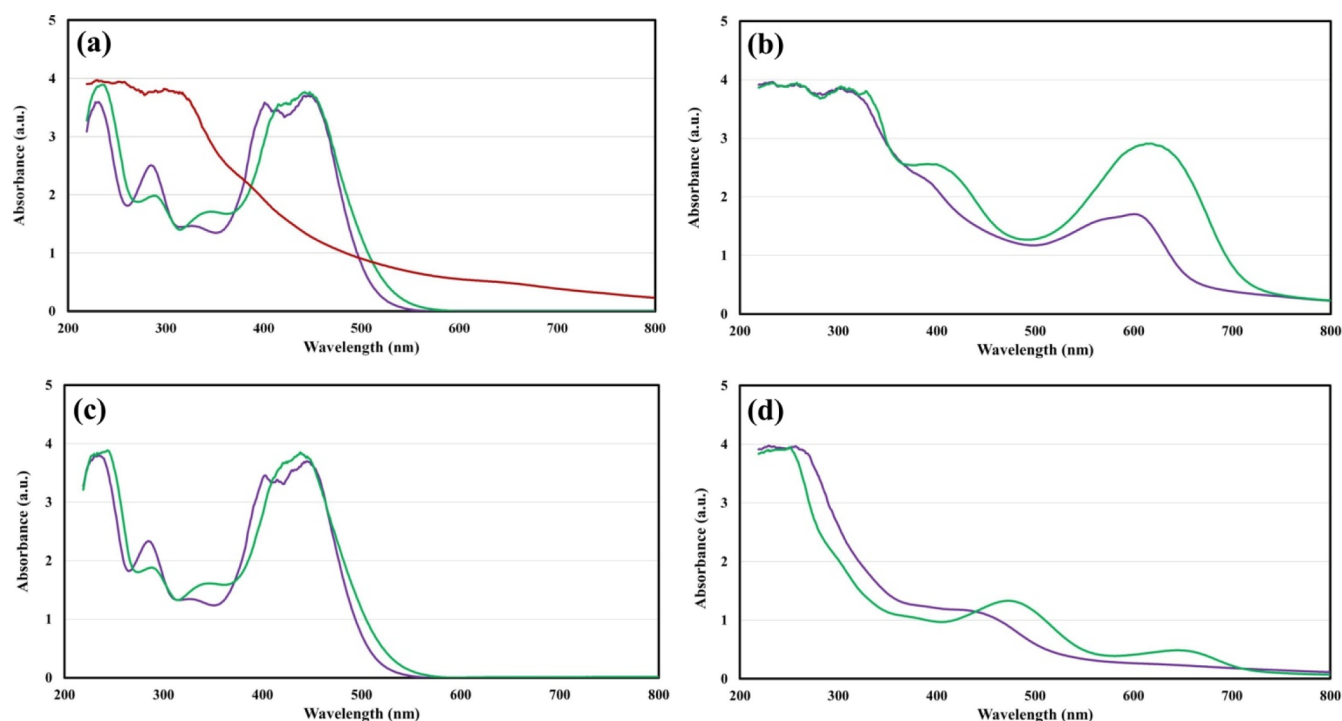
Figure 4. UV−vis spectra of (a) Alg/Ni−Al LDH (red ■), Alg/BP (purple ■) and Alg/BG (green ■), (b) Alg/Ni−Al LDH/BP (purple ■) and Alg/Ni−Al LDH/BG (green ■), (c) Alg/BP + acetic acid (purple ■) and Alg/BG + acetic acid (green ■), and (d) Alg/Ni−Al LDH/BP + acetic acid (purple ■) and Alg/Ni−Al LDH/BG + acetic acid (green ■).

incompatibility with other components. In the next step, the effect of increasing the color on the transparency of the film was investigated. According to Figure S3b, the film containing 1 mL of BP has the highest transparency of about 21% at 400 nm. Finally, the effect of the presence of LDH nanosheets in amounts of 5 to 8 mL was investigated. In general, the increase of LDH nanosheets caused a decrease in transparency; however, the film containing 6 mL of the LDH suspension has a transparency of about 5%, which was higher than that of other samples of the same category. LDH nanosheets are expected to increase transparency due to their placement to the wavelength of visible light.[22] However, this effect has not been observed, probably due to the accumulation (or agglomeration) of LDH nanosheets on each other and the formation of bonded phases inside the LDH and alginate networks.

2.2. Color Response. The optimization of time was investigated in the period of 10 to 70 min. Among the dyes used, only two samples BP and BG were sensitive to acetic acid, and the other dyes did not show any change in the presence of the analyte. Therefore, the results related to two dyes BP and BG were presented. The test results of Alg/Ni−Al LDH/BP composite films are shown in Figure 3a. The time of 60 min was used as the optimum for other steps. The long duration of the test can be related to the slow penetration of gas into the intermediate layers of the composite. As reported by Yu et al.,[18] inorganic LDH nanosheets effectively block the transport of small molecules. By making a composite based on polymers/inorganic nanosheets, the gas molecules are forced to rotate around the LDH nanosheets to diffuse through the film. This leads to a very tortuous and therefore a longer pathway. In this way, by controlling the arrangement of LDH nanosheets as a filler of alginate-based polymer films, the intensity and extent of pollutant penetration can be controlled over time. The results of Alg/Ni−Al LDH/BG composite films are shown in Figure 3a.

As can be seen, both composites have similar behavior, which can be related to the presence of LDH nanosheets.

Figure 3b shows the effect of % RH on the sensitivity of the colorimetric sensor. According to the results obtained in the previous step, the measurement was done in 60 min and 3.5 ppm. As can be seen from the graph, the sensitivity was almost independent of the % RH level. In other words, the sensor has good resistance to humidity, which is consistent with the results obtained for chemiresistive gas sensors.[15] This can be attributed to the presence of interlayer water molecules in the LDH structure. It is possible to say that the construction of the sensor using a simple casting method along with the controlled arrangement of the dye molecules has enabled us to make a stable sensor against humidity in order to detect the breath volatile cancer marker. So, at higher % RH values, BP and BG have shown a maximum sensitivity change of one unit. This lack of influence of % RH on the sensitivity can be very useful for measuring acetic acid as a breath volatile cancer marker because in this case, the response of the sensor will be independent of % RH. Also, Figure 3b shows images of sensors before (I) and after (II) acetic acid exposure with MATLAB program output.

Figure 3c shows the calibration curves obtained for Alg/Ni−Al-LDH/dye composite films. In both cases, sensitivity increased linearly with the acetic acid concentration. The BP-based sensor has a slowly increasing slope in the range of 0.5−2 ppm, while the BG-based sensor has an increasing slope in the entire concentration range. In order to investigate the response behavior more precisely, the line equation and the R^2 of the sensors made with different LDH values for the two dyes (BP and BG) are shown in Table S1. The results related to BP and BG have a R^2 between 0.92−0.98 and 0.79−0.92, respectively. It was found that the Alg/Ni−Al-LDH/BP composite at the value of LDH equal to 6 mL has a higher sensitivity and a lower R^2 than other samples. However, because it has a higher quality in
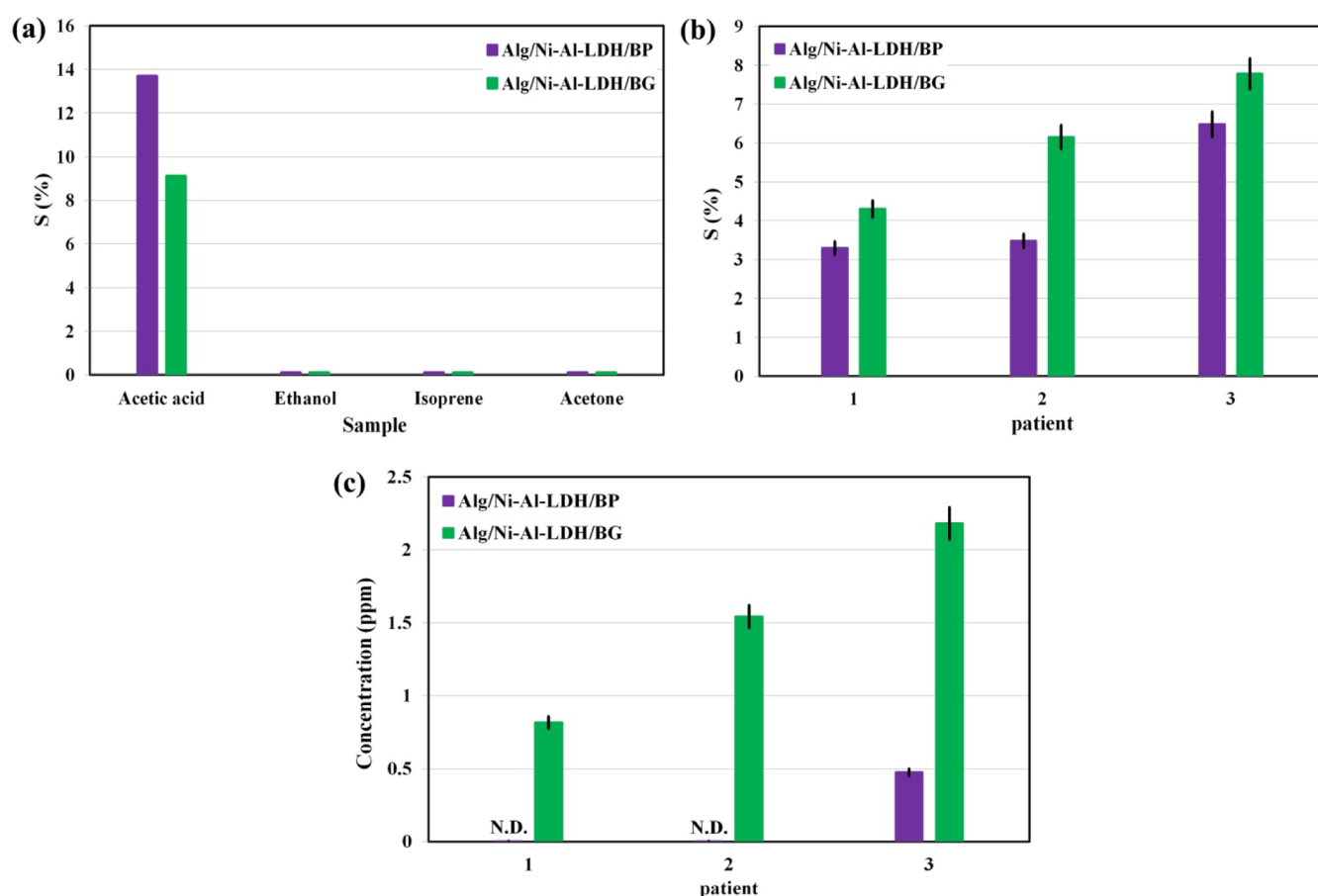
Figure 5. (a) Selectivity of Alg/Ni−Al-LDH/dye composite films [at 40% RH, time 60 min, and ambient temperature (purple ■ BP and green ■ BG)], (b) real sample test of the colorimetric sensor based on Alg/Ni−Al-LDH/dye composite films [at 90% RH, time 60 min, and ambient temperature (purple ■ BP and green ■ BG)], and (c) extrapolated analyte concentration [N.D.: no detection] {the sensor response [S_{RGB} (%) = S (%)]}.

terms of mechanical and appearance properties, it was used for other steps.

Repeatability and reproducibility in fabrication and sensitivity to the analyte were examined as one of the functional characteristics of the sensors and were measured under optimal conditions (Figure 3d). Table S2 shows the order sensors' sensitivity along with the calculated numerical values including mean ($\overline{X}$), standard deviation (s), RSD, LOD, and LOQ. Figure 3d shows images of sensors before (I) and after (II) acetic acid exposure with the MATLAB program output. As can be seen, the sensors have good response stability. The sensors have a closed error bar range, in addition to good reproducibility in manufacturing and measurement (Figure 3d). This case shows the usability of sensors in practical applications.

Figure 4 shows the UV−vis absorption spectrum of dye solutions and Ni−Al-LDH, individually and together. Dye solutions were prepared with a concentration of 3×10^{-3} M in ethanol. The Ni−Al-LDH suspension was the product of refluxing for 24 h at 120 °C and ultrasonication (50 kHz) for 5 h. The UV−vis spectrum of Ni−Al-LDH has a strong absorption in the range below 300 nm, which is a characteristic of Ni−Al-LDH nanosheets.[16] After that, the absorption in the range of 320 nm decreased with a gentle slope, which was consistent with the results presented by Jiao et al.[16] and Zhang et al.[17] BP and BG solutions have three and four characteristic peaks at wavelengths of about "285, 400, and 445 nm" and "290, 340, 415, and 440 nm", respectively. The mixture of the dye solution with the Ni−

Al-LDH suspension causes the shift and quenching of the absorption peak (transmittance increase), so the peaks below 350 nm are affected by the Ni−Al-LDH nanosheets. Figure 4b shows two peaks in the range of 395 and 605 nm for BP and two peaks in the range of 405 and 620 nm for BG. Taking a closer look at Figure 4a, dye solutions have a broad peak in the range of 360 to 480 nm (the peak widths at half-height). A red shift and a blue shift occur after the addition of Ni−Al-LDH nanosheets (Figure 4b).

For Ni−Al-LDH/BP, it has been observed that the peak at 400 nm shifts to 395 nm (blue shift, H-type) and the peak at 445 nm shifts to 605 nm (red shift, J-type). This was also observed for Ni−Al-LDH/BG and the displacements were almost similar for both peaks. According to the explanation of Jiao et al.,[16] the results observed can be related to the aggregation states of dye molecules in composite films. In the next step, the effect of acetic acid's presence in the solution was investigated (Figure 4c,d). Acetic acid did not affect the solution of BP and BG dyes (Figure 4c). However, on comparing Figure 4b,d, it can be seen that the characteristic peaks shift to a significant level.

- Ni−Al-LDH/BP: the broad peak in the region of 550−650 nm was completely quenched, and no other absorption peak was observed in the region above 400 nm.

- Ni−Al-LDH/BG: the proximity of the composite with acetic acid leads to the shift of the peaks in the regions of 405 and 620 to 475 and 650 nm, respectively (red shift).
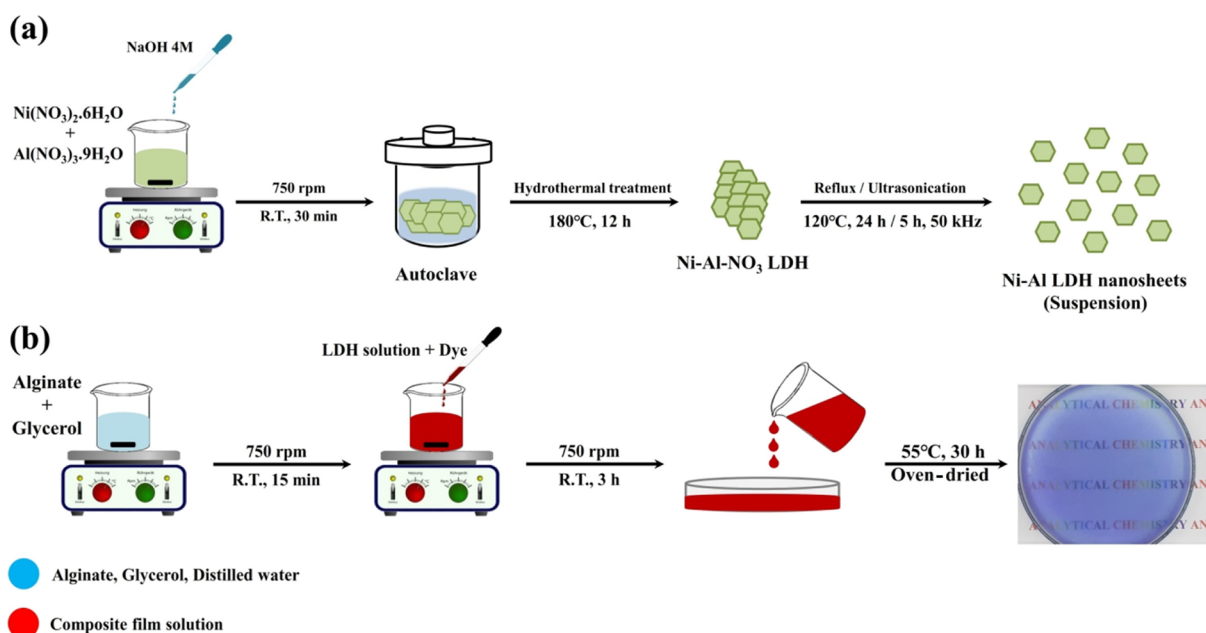
Figure 6. Schematic of the (a) Ni−Al LDH nanosheet and (b) Alg/Ni−Al-LDH/dye composite film synthesis method.

Selectivity and real sample tests were conducted as supplementary tests to investigate the performance of the sensors. As stated in the Introduction, mainly selected-ion flow-tube mass spectrometry or PTR-MS methods are used for breath testing.[1,36] These methods, in addition to being expensive and requiring trained personnel, have a low LOD and excellent detection selectivity. However, the development of noninvasive methods is inevitable and vital. According to the literature, human breath is a complex collection of different VOCs, each of which expresses a specific characteristic.[4] For example, ammonia in the breath can be associated with asthma, chronic renal failure/uremia, gastrointestinal disease, halitosis, and pulmonary arterial hypertension.[1] The pH indicators react with both acidic and basic compounds, and their color changes. It should be noted that the colors used include BP and BG, which have pH ranges of the color change of 3.8−5.4 (yellow to blue) and 5.2−6.8 (yellow to purple), respectively. According to the content expressed, the color molecules in the prepared composite film are in their higher pH range. In other words, BP and BG dye molecules are located at pH 5.4 (blue) and 6.8 (purple), respectively. Therefore, the presence of a strong base such as ammonia will not be able to change the color of the film, which is consistent with the experimental results obtained (results not presented here).

Therefore, it can be said that the presence of ammonia in breathing will be the main obstacle to measuring acetic acid as a breath marker of gastrointestinal disease. To solve this problem, a sensor array was used to measure the real sample (two test sets, one for ammonia and the other for acetic acid). The experiment was carried out under optimal conditions. The selectivity of the sensors in the presence of ethanol, isoprene, and acetone gases was investigated according to Pineau et al.[36] According to the obtained results, the sensors did not provide any response to the measured gases except for acetic acid (Figure 5a). In the following, real sample testing was performed on people with chronic gastrointestinal diseases. (Note: the ammonia sensor used was the same BP- and BG-based composite without LDH nanosheets.) Figure 5b shows the results. The analyte concentration was obtained by the extrapolation of the

calibration curve (3.5 ppm of acetic acid). As shown in Figure 5c, the Alg/Ni−Al-LDH/BG composite has a higher detection capability than the Alg/Ni−Al-LDH/BP composite. This means that among the three tested patients with acute conditions of gastric reflux disease, the Alg/Ni−Al-LDH/BG composite was able to detect acetic acid in the patient's breath in all three cases, while the Alg/Ni−Al-LDH/BP composite only detected the analyte in the third patient. It is necessary to point out that the sensors made in the presence of other pH indicators mentioned in Sections 2 and 4.1 Materials did not show any response to acetic acid. Therefore, it can be stated that despite their disadvantages, the constructed sensors have practical capabilities in measuring breath volatile cancer markers in an array form.

3. CONCLUSIONS

Colorimetric methods are simple and low-cost due to the use of indicator dyes as the basic units of a colorimetric sensor array. Here, the fabrication of colorimetric sensor films based on alginate as a polysaccharide was studied by the solution casting method. Alginate-based biopolymer films have provided efficient sensors with high flexibility by forming an egg-box structure and cross-linking Ni−Al-LDH nanosheets with a pH indicator. In composite films, LDH nanosheets can cause the aggregation of different dye molecules in the form of J- and/or H-arrangement. The obtained results indicate the construction of a dedicated sensor array for the quantitative and qualitative measurement of acetic acid as a breath volatile cancer marker. High response time (60 min) was one of the most important problems of the presented sensors. However, the presented functional capabilities clear the way for the development of noninvasive sensors. It is also expected to be used as a promising chemical sensor.

4. MATERIALS AND METHODS

4.1. Materials. Sodium alginate [Alg, chemically pure, viscosity (2%, 25 °C)] was purchased from Sigma-Aldrich. Other materials include nickel(II) nitrate hexahydrate [Ni-(NO$_3$)$_2$·6H$_2$O], aluminum nitrate nonahydrate [Al(NO$_3$)$_3$·

9H$_2$O], sodium hydroxide (NaOH), glycerol (C$_3$H$_8$O$_3$), BP (C$_{21}$H$_{16}$Br$_2$O$_5$S), bromothymol blue (C$_{27}$H$_{28}$Br$_2$O$_5$S) (b-TB), thymol blue (C$_{27}$H$_{30}$O$_5$S) (TB), methyl red (C$_{15}$H$_{15}$N$_3$O$_2$) (MR), phenol red (C$_{19}$H$_{14}$O$_5$S) (PR), *m*-cresol purple (C$_{21}$H$_{18}$O$_5$S) (*m*-CP), methyl orange (C$_{14}$H$_{14}$N$_3$NaO$_3$S) (MO), and BG (C$_{21}$H$_{14}$Br$_4$O$_5$S) were purchased from Merck. All the chemicals were of analytical grade and were used without purification. All aqueous solutions were prepared with high-purity deionized water (nitrate slats) and absolute ethanol (dyes).

4.2. LDH Nanosheet Preparation. In this method, 2.923 g of Ni(NO$_3$)$_2$·6H$_2$O with 1.704 g of Al(NO$_3$)$_3$·9H$_2$O (with a molar ratio of 2:1) were dissolved in 20 mL of distilled water. In this case, the final concentrations were 8 and 4 mM, respectively.[19,20] Then, a 4 M NaOH solution was added dropwise to the above solution. The pH of the solution was adjusted to 10 by adding a NaOH solution. The obtained colloidal solution was sealed in a Teflon-lined stainless-steel autoclave and kept at 180 °C for 12 h. The green sediment obtained after separation by a centrifuge was washed with distilled water and ethanol and placed at 70 °C for 4 h to dry. To create LDH nanosheets, 1 g of the dry LDH sediment was added to 100 mL of distilled water. After purging with N$_2$ gas, the mixture was refluxed for 24 h at 120 °C. The mixture was immediately treated with ultrasonic waves (50 kHz) for 5 h at 60 °C. The LDH nanosheets were separated by centrifugation under conditions of 3000 rpm for 10 min.

4.3. Film Preparation. The films were prepared by the solution casting method. 1 g of sodium alginate was added to 100 mL of distilled water containing 0.5 g of glycerol under vigorous mixing. Glycerol was used as a plasticizer to increase flexibility and reduce the brittleness of the final film. 60 mL of the mixture obtained after filtration (by fustian fabric) was mixed with 7 mL of a solution containing LDH nanosheets (obtained from the previous step) and 1 mL of the homogeneous dye solution for 3 h. The homogeneous suspension was poured onto a Petri dish (10 × 10 cm^2) and dried for 30 h at 55 °C in an oven. The prepared films were placed on double-sided adhesive tape with a white background. Figure 6a,b shows a schematic representation of the synthesis process used in Ni−Al LDH nanosheets and the Alg/Ni−Al-LDH/dye composite, respectively. The LDH solution in amounts of 2 to 10 mL and an alcoholic solution of BP dye in volumes of 0.5 to 2 mL were used and optimized. Also, the response of MR, PR, TB, b-TB, *m*-CP, MO, and BG was investigated. [The schematic and description of the Alg/Ca^{2+}/Ni−Al LDH composite (Figure S1) synthesis method are given in the Supporting Information. As can be seen, the color of the final film was different in the presence and absence of calcium ions.]

4.4. Characterization. The characterization section is presented in the Supporting Information.

ASSOCIATED CONTENT

Ⓢ Supporting Information

The Supporting Information is available free of charge at https://pubs.acs.org/doi/10.1021/acsomega.3c01617.

> Synthesis of the Alg/Ca^{2+}/Ni−Al-LDH/dye composite; characterization of composites including XRD, FESEM, UV−vis, FTIR spectroscopy, AFM, tensile strength and EAB, light transmittance, acetic acid sensing chamber, image processing and color stability; visual and

mechanical characteristics of films; and statistical characteristics (PDF)

AUTHOR INFORMATION

Corresponding Authors

M. Hassan Amini − *Faculty of Clean Technologies, Chemistry and Chemical Engineering Research Center of Iran, Tehran 1497716320, Iran;* ⊙ orcid.org/0000-0003-3924-1015; Email: amini@ccerci.ac.ir

S. Hamid Ahmadi − *Faculty of Clean Technologies, Chemistry and Chemical Engineering Research Center of Iran, Tehran 1497716320, Iran;* Email: ahmadi@ccerci.ac.ir

Author

S. Amirabbas Zakaria − *Faculty of Clean Technologies, Chemistry and Chemical Engineering Research Center of Iran, Tehran 1497716320, Iran*

Complete contact information is available at:
https://pubs.acs.org/10.1021/acsomega.3c01617

Notes

REFERENCES

(1) Broza, Y. Y.; Vishinkin, R.; Barash, O.; Nakhleh, M. K.; Haick, H. Synergy between nanomaterials and volatile organic compounds for non-invasive medical evaluation. *Chem. Soc. Rev.* **2018**, *47*, 4781−4859.

(2) Haick, H.; Broza, Y. Y.; Mochalski, P.; Ruzsanyi, V.; Amann, A. Assessment, origin, and implementation of breath volatile cancer markers. *Chem. Soc. Rev.* **2014**, *43*, 1423−1449.

(3) Adiguzel, Y.; Kulah, H. Breath sensors for lung cancer diagnosis. *Biosens. Bioelectron.* **2015**, *65*, 121−138.

(4) Pauling, L.; Robinson, A. B.; Teranishi, R.; Cary, P. Quantitative Analysis of Urine Vapor and Breath by Gas-Liquid Partition Chromatography. *Proc. Natl. Acad. Sci. U.S.A.* **1971**, *68*, 2374−2376.

(5) Fenske, J. D.; Paulson, S. E. Human Breath Emissions of VOCs. *J. Air Waste Manage. Assoc.* **1999**, *49*, 594−598.

(6) Jalal, A.; Alam, F.; Roychoudhury, S.; Umasankar, Y.; Pala, N.; Bhansali, S. Prospects and challenges of volatile organic compound (VOC) sensors in human healthcare. *ACS Sens.* **2018**, *3*, 1246−1263.

(7) Kang, N. K.; Jun, T. S.; La, D. D.; Oh, J. H.; Cho, Y. W.; Kim, Y. S. Evaluation of the limit-of-detection capability of carbon black-polymer composite sensors for volatile breath biomarkers. *Sens. Actuators, B* **2010**, *147*, 55−60.

(8) Wang, D.; Zhang, F.; Prabhakar, A.; Qin, X.; Forzani, E. S.; Tao, N. Colorimetric Sensor for Online Accurate Detection of Breath Acetone. *ACS Sens.* **2021**, *6*, 450−453.

(9) Zhao, S.; Lei, J.; Huo, D.; Hou, C.; Luo, X.; Wu, H.; Fa, H.; Yang, M. A colorimetric detector for lung cancer related volatile organic compounds based on cross-response mechanism. *Sens. Actuators, B* **2018**, *256*, 543−552.

(10) Kim, K. H.; Jahan, S. A.; Kabir, E. A review of breath analysis for diagnosis of human health. *TrAC, Trends Anal. Chem.* **2012**, *33*, 1−8.

(11) Li, J.; Hou, C.; Huo, D.; Yang, M.; Fa, H.; Yang, P. Development of a colorimetric sensor Array for the discrimination of aldehydes. *Sens. Actuators, B* **2014**, *196*, 10−17.

(12) Mustafa, F.; Carhart, M.; Andreescu, S. A 3D-Printed Breath Analyzer Incorporating CeO$_2$ Nanoparticles for Colorimetric Enzyme-Based Ethanol Sensing. *ACS Appl. Nano Mater.* **2021**, *4*, 9361−9369.

(13) Nie, L.; Fan, G.; Wang, A.; Zhang, L.; Guan, J.; Han, N.; Chen, Y. Finely dispersed and highly toluene sensitive NiO/NiGa$_2$O$_4$ heterostructures prepared from layered double hydroxides precursors. *Sens. Actuators, B* **2021**, *345*, 130412.

(14) Morandi, S.; Prinetto, F.; Di Martino, M.; Ghiotti, G.; Lorret, O.; Tichit, D.; Malagu, C.; Vendemiati, B.; Carotta, M. C. Synthesis and

characterisation of gas sensor materials obtained from Pt/Zn/Al layered double hydroxides. *Sens. Actuators, B* **2006**, *118*, 215−220.

(15) Zakaria, S. A.; Ahmadi, S. H.; Amini, M. H. Chemiresistive gas sensors based on layered double hydroxides (LDHs) structures: A review. *Sens. Actuators, A* **2022**, *346*, 113827.

(16) He, Y.; Wang, R.; Jiao, T.; Yan, X.; Wang, M.; Zhang, L.; Bai, Z.; Zhang, Q.; Peng, Q. Facile Preparation of Self-Assembled Layered Double Hydroxide-Based Composite Dye Films As New Chemical Gas Sensors. *ACS Sustainable Chem. Eng.* **2019**, *7*, 10888−10899.

(17) He, Y.; Wang, R.; Sun, C.; Liu, S.; Zhou, J.; Zhang, L.; Jiao, T.; Peng, Q. Facile Synthesis of Self-Assembled NiFe Layered Double Hydroxide-Based Azobenzene Composite Films with Photoisomerization and Chemical Gas Sensor Performances. *ACS Omega* **2020**, *5*, 3689−3698.

(18) Yu, J.; Liu, J.; Clearfield, A.; Sims, J. E.; Speiegle, M. T.; Suib, S. L.; Sun, L. Synthesis of Layered Double Hydroxide Single-Layer Nanosheets in Formamide. *Inorg. Chem.* **2016**, *55*, 12036−12041.

(19) Shu, Y.; Yin, P.; Wang, J.; Liang, B.; Wang, H.; Guo, L. Bioinspired Nacre-like Heparin/Layered Double Hydroxide Film with Superior Mechanical, Fire-Shielding, and UV-Blocking Properties. *Ind. Eng. Chem. Res.* **2014**, *53*, 3820−3826.

(20) Shu, Y.; Yin, P.; Liang, B.; Wang, S.; Gao, L.; Wang, H.; Guo, L. Layer by layer assembly of heparin/layered double hydroxide completely renewable ultrathin films with enhanced strength and blood compatibility. *J. Mater. Chem.* **2012**, *22*, 21667.

(21) Fang, Y.; Al-Assaf, S.; Phillips, G. O.; Nishinari, K.; Funami, T.; Williams, P. A. Binding behavior of calcium to polyuronates: Comparison of pectin with alginate. *Carbohydr. Polym.* **2008**, *72*, 334−341.

(22) Liang, B. L.; Wang, J. F.; Shu, Y.; Yin, P. G.; Guo, L. A biomimetic ion-crosslinked layered double hydroxide/alginate hybrid film. *RSC Adv.* **2017**, *7*, 32601−32606.

(23) Wang, Q.; O'Hare, D. Recent Advances in the Synthesis and Application of Layered Double Hydroxide (LDH) Nanosheets. *Chem. Rev.* **2012**, *112*, 4124−4155.

(24) Yan, L.; Wang, Y.; Li, J.; Kalytchuk, S.; Susha, A. S.; Kershaw, S. V.; Yan, F.; Rogach, A. L.; Chen, X. Highly luminescent covalently bonded double hydroxide nanoparticle-fluorescent dye nanohybrids. *J. Mater. Chem. C* **2014**, *2*, 4490−4494.

(25) Huang, S.; Cen, X.; Zhu, H.; Yang, Z.; Yang, Y.; Tjiu, W. W.; Liu, T. Facile preparation of poly(vinyl alcohol) nanocomposites with pristine layered double hydroxides. *Mater. Chem. Phys.* **2011**, *130*, 890−896.

(26) Rahman, M. T.; Kameda, T.; Kumagai, S.; Yoshioka, T. A novel method to delaminate nitrate-intercalated MgeAl layered double hydroxides in water and application in heavy metals removal from waste water. *Chemosphere* **2018**, *203*, 281−290.

(27) Karimi Khorrami, N.; Radi, M.; Amiri, S.; McClements, D. J. Fabrication and characterization of alginate-based films functionalized with nanostructured lipid carriers. *Int. J. Biol. Macromol.* **2021**, *182*, 373−384.

(28) Zheng, H.; Yang, J.; Han, S. The synthesis and characteristics of sodium alginate/graphene oxide composite films crosslinked with multivalent cations. *J. Appl. Polym. Sci.* **2016**, *133*, 43616.

(29) Ravuru, S. S.; Jana, A.; De, S. Synthesis of NiAl-layered double hydroxide with nitrate intercalation: application in cyanide removal from steel industry effluent. *J. Hazard. Mater.* **2019**, *373*, 791−800.

(30) Liang, B.; Wang, J.; Shu, Y.; Yin, P.; Guo, L. A biomimetic ion-crosslinked layered double hydroxide/alginate hybrid film. *RSC Adv.* **2017**, *7*, 32601−32606.

(31) Podsiadlo, P.; Kaushik, A. K.; Arruda, E. M.; Waas, A. M.; Shim, B. S.; Xu, J.; Nandivada, H.; Pumplin, B. G.; Lahann, J.; Ramamoorthy, A.; Kotov, N. A. Ultrastrong and Stiff Layered Polymer Nanocomposites. *Science* **2007**, *318*, 80−83.

(32) Ming, P.; Song, Z.; Gong, S.; Zhang, Y.; Duan, J.; Zhang, Q.; Jiang, L.; Cheng, Q. Nacre-inspired Integrated Nanocomposites with Fire Retardant Properties by Graphene Oxide and Montmorillonite. *J. Mater. Chem. A* **2015**, *3*, 21194−21200.

(33) Lan, W.; He, L.; Liu, Y. Preparation and Properties of Sodium Carboxymethyl Cellulose/Sodium Alginate/Chitosan Composite Film. *Coatings* **2018**, *8*, 291.

(34) Liang, B.; Zhao, H.; Zhang, Q.; Fan, Y.; Yue, Y.; Yin, Pe.; Guo, L. Ca^{2+} Enhanced Nacre-Inspired Montmorillonite-Alginate Film with Superior Mechanical, Transparent, Fire Retardancy, and Shape Memory Properties. *ACS Appl. Mater. Interfaces* **2016**, *8*, 28816−28823.

(35) Wang, G.; Rao, D.; Li, K.; Lin, Y. UV Blocking by Mg−Zn−Al Layered Double Hydroxides for the Protection of Asphalt Road Surfaces. *Ind. Eng. Chem. Res.* **2014**, *53*, 4165−4172.

(36) Pineau, N. J.; Krumeich, F.; Güntner, A. T.; Pratsinis, S. E. Y-doped ZnO films for acetic acid sensing down to ppb at high humidity. *Sens. Actuators, B* **2021**, *327*, 128843.